

High-Performance, Stretchable, Wire-Shaped Supercapacitors**

Tao Chen, Rui Hao, Huisheng Peng, and Liming Dai*

Abstract: A general approach toward extremely stretchable and highly conductive electrodes was developed. The method involves wrapping a continuous carbon nanotube (CNT) thin film around pre-stretched elastic wires, from which high-performance, stretchable wire-shaped supercapacitors were fabricated. The supercapacitors were made by twisting two such CNT-wrapped elastic wires, pre-coated with poly(vinyl alcohol)/H₃PO₄ hydrogel, as the electrolyte and separator. The resultant wire-shaped supercapacitors exhibited an extremely high elasticity of up to 350% strain with a high device capacitance up to 30.7 F g⁻¹, which is two times that of the state-of-the-art stretchable supercapacitor under only 100% strain. The wire-shaped structure facilitated the integration of multiple supercapacitors into a single wire device to meet specific energy and power needs for various potential applications. These supercapacitors can be repeatedly stretched from 0 to 200% strain for hundreds of cycles with no change in performance, thus outperforming all the reported state-of-the-art stretchable electronics.

Stretchable electronics with unchanging performance, even under high tensile strain or large deformation, have recently attracted increasing attention because of their multifunctional applications, which range from wearable units through biomedical devices to energy systems. Stretchable conductive electrodes with a high elasticity and good conductivity are essential for fabricating various stretchable optoelectronic devices, including supercapacitors^[1,2] and batteries^[3] for energy storage, polymer solar cells,^[4,5] and OLEDs^[6] for energy conversion, and transistors.^[7,8] Stretchable conductive electrodes with planar geometries based on carbon nanomaterials (e.g., nanotubes,^[1,2,9] graphene^[10,11]), metal nanowires,^[12] metal nanoparticles,^[13] or conductive polymers,^[14] have been devised for devices for energy storage and conversion.^[1,2,9,10] However, most of the reported stretchable electrodes have a low elasticity (<100%), which limits performance of the resultant electronic devices.^[9–14] It remains a great challenge to develop highly elastic wire-

shaped electronics because most of the existing wires are either stretchable, but nonconductive (e.g., elastic polymer fibers), or vice versa (e.g., metal wires). A few studies on stretchable conductive wires have been reported,^[15,16] whereas the development of stretchable wire-shaped electronics has been much less discussed in the literature. However, if such electronics (e.g., supercapacitors) are realized, they could be very useful as power sources for various miniaturized electronic devices, ranging from micro-robots, through wearable electronic textiles, to integrated energy conversion and storage systems.^[17–19] Furthermore, stretchable wire-shaped electronics can be easily integrated into unconventional substrates (e.g., human skin and lenses^[20]), which play critical roles in biointerfacing with electronic skins^[21–24] and tuning dynamics of such devices as electronic lasers and eye cameras.^[25,26] Very recently, Yang et al. have, for the first time, demonstrated a stretchable wire-shaped supercapacitor with a coaxial structure and it maintained its electrochemical performance up to a strain of 80%.^[27] To date, all the reported stretchable supercapacitors with either planar or wire-shaped structures showed limited elasticities (below 120%).^[1,2,27]

By wrapping a continuous CNT thin film around pre-stretched elastic wires, containing 64% polyester and 36% polyurethane (Gütermann Company) with different pre-strain (30%, 60%, and 100%; Figure 1), we developed conductive wires with an extremely high elasticity and high conductivity, even up to 300% strain, and is thus higher than that of any other stretchable conducting wires reported previously.^[18,19] Extremely elastic wire-shaped supercapacitors were fabricated by twisting two such CNT-wrapped elastic wires, pre-coated with poly(vinyl alcohol) powder (PVA)/H₃PO₄/water (10 g/10 g/100 mL) hydrogel, as the electrolyte and separator. The wire-shaped supercapacitors remained undamaged and there was almost no change in capacitive performance even under stretching up to 350% strain, and it is more than two times strain variation than that previously reported.^[27]

Figures 1a,b schematically show the route to the CNT-wrapped stretchable and conductive wires. To start with, an elastic wire was fixed on two supports, then stretched to a pre-determined strain, ranging from 30 to 100%. Then, the aligned CNT sheet is directly drawn from a vertically aligned CNT (VA-CNT) array^[28–30] and simultaneously wrapped around the pre-stretched wire while it was rotated backwards and forwards by hand. The VA-CNT array was synthesized by chemical vapor deposition according to the previously reported procedure.^[28–30] Figure S1a (see the Supporting Information) shows a digital photograph of the process for drawing the CNT film from a VA-CNT array on a Si substrate, and continuously wrapping the CNT sheet around the elastic wire. Upon releasing the pre-stretched wire to its natural

[*] Dr. T. Chen, Dr. R. Hao, Prof. L. Dai
Center of Advanced Science and Engineering for Carbon (Case4-Carbon), Department of Macromolecular Science and Engineering, Case Western Reserve University
10900 Euclid Avenue, Cleveland, OH 44106 (USA)
E-mail: liming.dai@case.edu

Prof. H. Peng
State Key Laboratory of Molecular Engineering of Polymers, Department of Macromolecular Science and Laboratory of Advanced Materials, Fudan University, Shanghai 200438 (China)

[**] This work was supported by AFOSR (FA-9550-12-1-0069), NSF (CMMI-1266295, AIR-IIP-1343270, DMR-1106160), and DAGSI.

Supporting information for this article is available on the WWW under <http://dx.doi.org/10.1002/anie.201409385>.

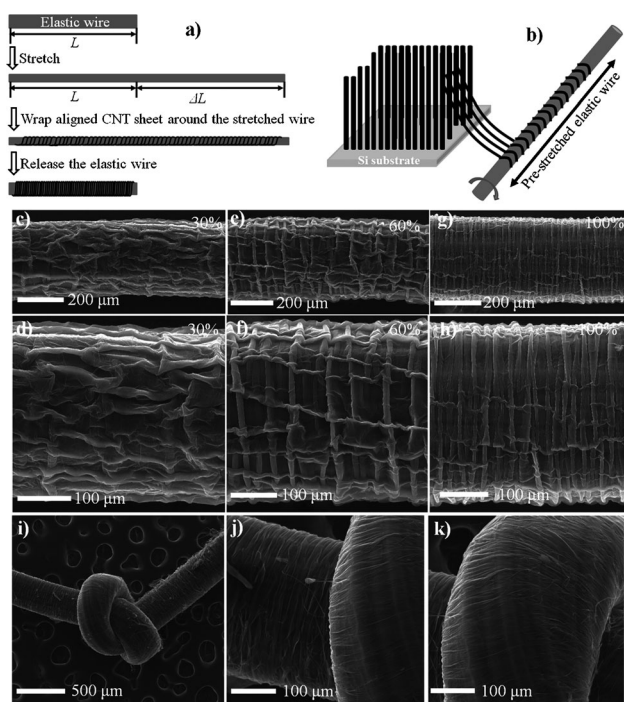


Figure 1. a,b) Schematic illustration of fabricating stretchable conducting wire by wrapping aligned CNT sheet around a pre-stretched elastic wire. Morphology and flexibility of the CNT-wrapped 64% polyester and 36% polyurethane elastic wire. SEM images of the buckled CNTs wrapped on the elastic wire with a 30% (c,d), 60% (e,f), and 100% (g,h) pre-strain. i–k) SEM images of a knot made from the CNT-wrapped elastic wire with a 100% pre-strain.

state, the CNT-wrapped elastic wire showed a buckling structure of highly overlapped CNT sheets in the coating layer (Figures 1c–h, and Figures S1 and S2 in the Supporting Information), which is different from the smooth CNT coating obtained by rotating the elastic wire in one direction without pre-stretching.^[27] The buckled CNT coating on the elastic wire facilitated the elasticity of the entire wire-shaped electrode up to an extremely high strain (> 300%) without detrimental effects to its electrical properties (see below).

Figures 1c–h show scanning electron microscope (SEM) images of the resultant elastic and conducting wires with buckled CNT coatings around the elastic wires of different pre-strains. The diameter for the starting elastic wires is 290 μm, around which a layer of about 10 μm thick aligned CNT sheet was wrapped (Figure 1c–h). The observed highly overlapped and buckled CNT coating imparted a high elasticity and electrical conductivity to the resultant wire electrodes. The buckling periodicity for the CNT coatings could be regulated by varying the applied pre-strains: decreasing from 100 μm through 50 μm to 20 μm as the applied pre-strains increased from 30%, through 60%, to 100% (Figure 1c–h). The resultant CNT-wrapped elastic wires are highly flexible and can even be tied in a knot (Figure 1i–k). It can be seen in Figure 1j and k that individual CNTs were highly aligned with each other inside the nanotube coating along the rotating direction.

We investigated the dependence of electrical resistance on the tensile strain. As seen in Figure S3 (see the Supporting

Information), the electrical resistance of the 100, 60, and 30% pre-stretched CNT-wrapped wires increased only by 30, 76, and 130%, respectively, when a tensile strain of 300% was applied, and is much better than any other stretchable wire electrodes reported previously.^[18,19]

The availability of these highly stretchable conductive wires prompted us to fabricate wire-shaped supercapacitors by twisting two of the CNT-wrapped elastic wires together with a PVA/H₃PO₄ gel electrolyte coating sandwiched between the twisted wire electrodes (Figure 2a,b; see the Supporting Information for detailed device fabrication).

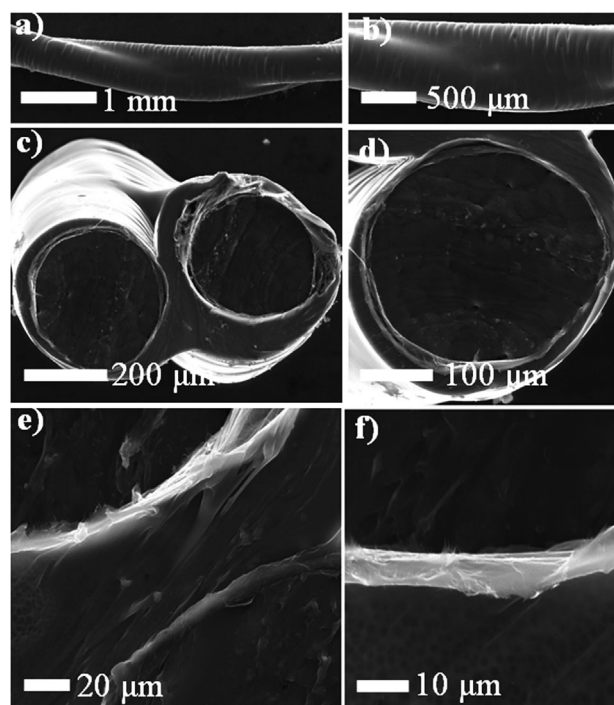


Figure 2. a,b) Top-view SEM images of the wire-shaped supercapacitor with a twisted structure under different magnifications. c,d) Cross-section SEM images of the twisted wire-shaped supercapacitor under different magnifications. e,f) Enlarged views of the region between the two twisted electrodes showing the electrolyte coating and CNT layers.

Figures 2c–f show cross-section SEM images of the twisted two-electrode supercapacitor, thus indicating about a 50 μm thick electrolyte coating between the two electrodes (Figure 2e) and a 10 μm thick CNT layer on each of the electrodes (Figure 2e and f). To further enhance the conductivity and capacitive performance, a thin layer of poly(3,4-ethylenedioxythiophene)/poly(styrene sulfonate), PEDOT-PSS, was coated onto the CNT-wrapped elastic wire electrodes before assembling them into a supercapacitor (Figure S2). Compared to a stretchable wire-shaped supercapacitor based on a single wire electrode with coaxial structure,^[27] the twisted two-electrode structure is mechanically stronger and hence can bare a much larger tensile force or deformation (see Figure S4 in the Supporting Information).

The electrochemical performance of the wire-shaped supercapacitor prepared from the two twisted CNT-wrapped elastic wires was evaluated by cyclic voltammetry (CV),

galvanostatic charge/discharge (GCD), and electrochemical impedance spectroscopy (EIS). Figure 3a shows CV curves measured at a scanning rate of 0.05 V s^{-1} for wire-shaped supercapacitors based on the bare CNT-wrapped and CNT/PEDOT-PSS-wrapped electrodes, respectively. The corresponding CV curves measured at different scanning rates from 0.02 to 0.1 V s^{-1} are given in Figure S5 (see the

thus indicating nearly ideal capacitive behaviors with a high Coulombic efficiency.^[34–37] From Figure 3b, specific capacitance of the entire cell (C_{cell}) based on the bare CNT-wrapped electrodes was calculated (see the Supporting Information) to be about 8.0 F g^{-1} at the discharge current of 0.5 A g^{-1} , which increased to 30.7 F g^{-1} for the CNT/PEDOT-PSS-wrapped electrodes and is about two times of that reported previously.^[27] The specific capacitance for the single CNT-wrapped and CNT/PEDOT-PSS-wrapped electrode (C_{single}) was 32.0 F g^{-1} and 122.8 F g^{-1} (Figure 3c), respectively, and are comparable to the corresponding non-elastic planar electrodes reported previously.^[31–33] As seen in Figure 3c, specific capacitances for all the twisted supercapacitors and single electrodes decreased gradually with increasing the current density because of a heavier polarization of the electrode at a higher current density.^[36,37]

Figure S6 (see the Supporting Information) shows Nyquist plots for supercapacitors based on both the bare CNT-wrapped and CNT/PEDOT-PSS-wrapped elastic wire electrodes recorded within a frequency range from 10^{-2} to 10^5 Hz . As can be seen, the device using the CNT/PEDOT-PSS-wrapped elastic wire electrodes possessed a lower series resistance and more vertical shape at low frequencies, and hence a better capacitive performance than the corresponding device using the bare CNT-wrapped elastic wire electrodes. These wire-shaped supercapacitors were further subjected to the capacitance cycle stability test. Figure 3d shows an excellent capacitance

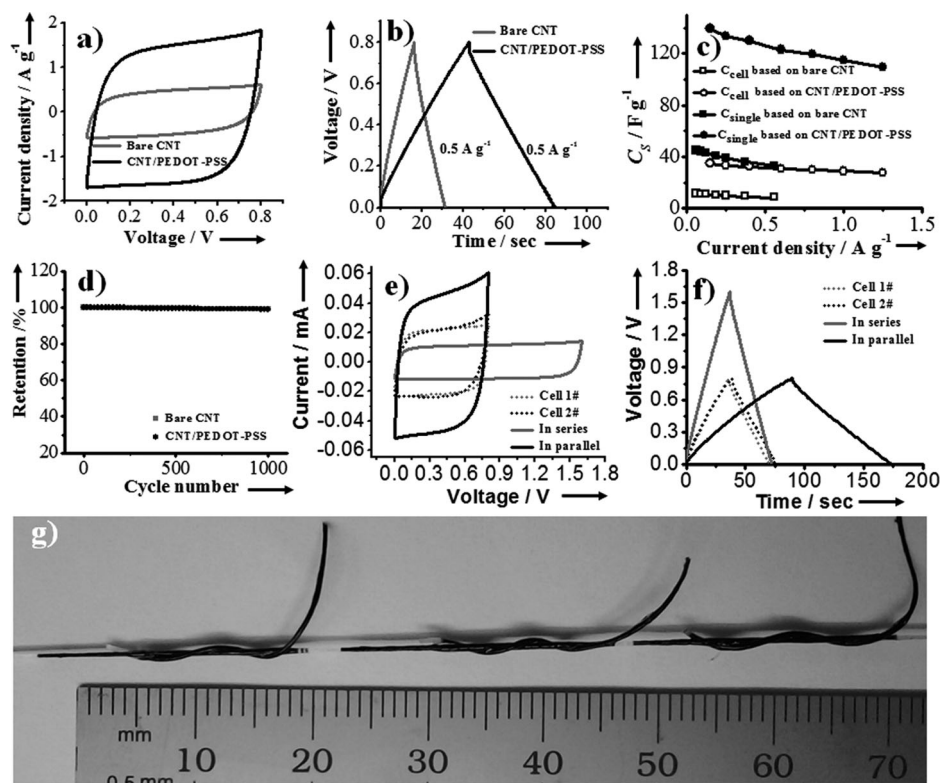


Figure 3. Electrochemical performance of the wire-shaped supercapacitors based on the bare CNT-wrapped and CNT/PEDOT-PSS-wrapped elastic wire electrodes. a) CV curves of the supercapacitors at a scan rate of 0.05 V s^{-1} . b) The galvanostatic charging-discharging curves of the supercapacitors at a constant current density of 0.5 A g^{-1} . c) Dependence of specific capacitance (C_s) on the discharging current density. d) Cycle stability of the supercapacitors at 0.5 A g^{-1} . e) CV curves for two individual cells and their integrated devices in series and in parallel recorded at a scanning rate of 0.05 V s^{-1} . f) GCD curves for two individual cells and their integrated devices in series and in parallel measured at a constant current of $10 \mu\text{A}$. g) Digital photograph of a wire integrating multiple supercapacitors using the bare CNT-wrapped electrodes, as exemplified by three of the supercapacitor cells.

Supporting Information). As can be seen, supercapacitors based on both the CNT-wrapped and CNT/PEDOT-PSS-wrapped electrodes showed nearly rectangular CV curves, thus indicating excellent capacitive behaviors. The highly conductive PEDOT-PSS coating could further enhance the capacitance of these CNT-wrapped wire-shaped supercapacitors because the oxygen-rich conjugated PEDOT-PSS should enhance both the ionic (electrolyte) and electronic charge transport.^[31–33] However, the corresponding supercapacitor based on a PEDOT-PSS-wrapped elastic wire electrode showed very poor performance because of poor elasticity of the PEDOT coating.

Figure 3b shows GCD curves with a typical symmetric triangular shape for supercapacitors based on both the CNT-wrapped and CNT-PEDOT-PSS-wrapped wire electrodes,

retention for supercapacitors based on both the bare CNT-wrapped and CNT/PEDOT-PSS-wrapped elastic wire electrodes with a only about a 1% decay in capacitance after 1000 charge/discharge cycles in both cases. Because of the wire-shaped structure, multiple supercapacitors can be easily integrated into a single wire device (Figure 3g) to meet specific energy and power needs for practical applications. As shown in Figure 3e and f, the charge/discharge voltage window was doubled when two individual devices were connected in series, while both the output current and discharge time increased by a factor of two when two devices were connected in parallel.

These wire-shaped supercapacitors also exhibited a good flexibility. As shown in Figure 4a–c, CV curves for the supercapacitors derived from both the CNT-wrapped and

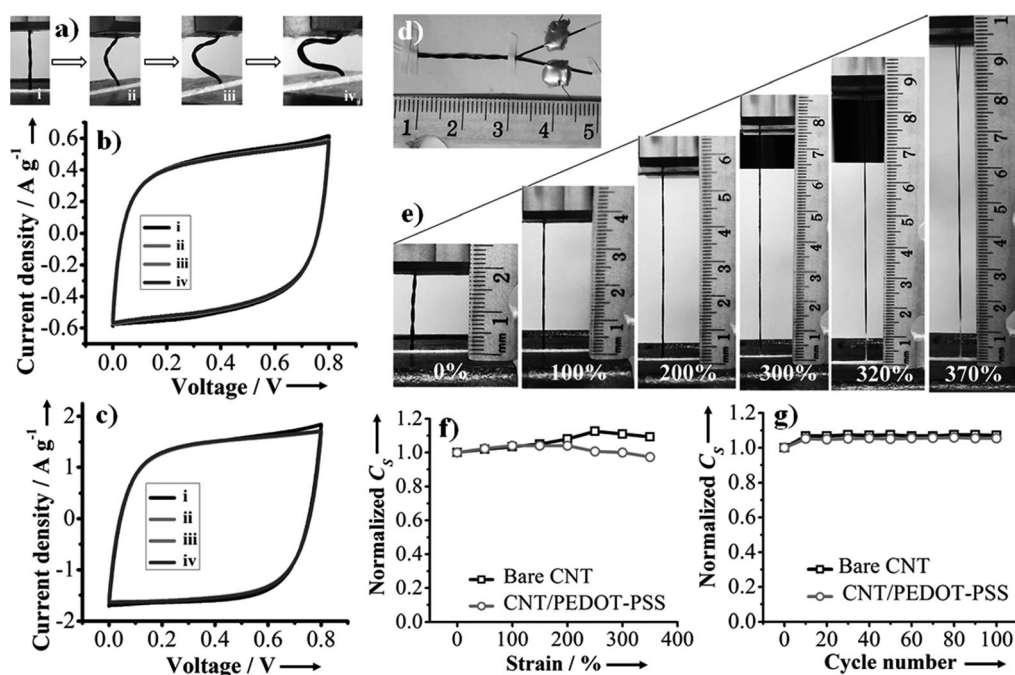


Figure 4. a) Digital photographs of the wire-shaped supercapacitors at different bending states. b,c) CV curves of the supercapacitors based on the bare CNT-wrapped (b) and CNT/PEDOT-PSS-wrapped (c) elastic wire electrodes under bending deformations at different bending states shown in (a). Digital photograph of a typical wire-shaped supercapacitor with a twisted structure before (d) and after (e) being stretched from strains of 0 to 370%. f) Changes in the normalized capacitance (C_s) as a function of the tensile strain. g) Changes in the normalized capacitance (C_s) as a function of the stretching cycle number; for each of the cycles the supercapacitor was stretched up to 200% strain and the strain was fully released at the end of each stretching.

CNT/PEDOT-PSS-wrapped elastic wire electrodes remained almost unchanged when they were bent to different states. As expected, the corresponding GCD curves did not show any significant change (see Figure S7 in the Supporting Information), thus indicating a high flexibility for these wire-shaped supercapacitors. Figure 4d shows a digital photograph of the twist wire-shaped supercapacitor with a copper wire being connected by silver paste onto each of the two twisted elastic wire electrodes for device performance measurements during the stretching in situ. Figure 4e shows digital photographs for the twisted wire-shaped supercapacitor under stretching from 0 to 370% strains. While Figures S8 and S9 (see the Supporting Information) show CV and GCD curves for the supercapacitors based on the CNT-wrapped and CNT-PEDOT-PSS-wrapped elastic wire electrodes, respectively, their specific capacitances at different tensile strains are summarized in Table S1 (see the Supporting Information). Figure 4f shows the normalized capacitance (i.e., a ratio of the capacitance under a specific strain to that at 0 strain) as a function of the tensile strain. As can be seen in Figure 4f, the capacitance for the device based on the bare CNT-wrapped elastic wire electrodes increased by 13% as the tensile strain increased from 0 to 250%, presumably because of the strain-induced enhancement in the contact between the two twisted electrodes upon stretching.^[2,27] Further stretching beyond the 250% strain caused a slight decrease in the capacitance associated with possible deformation of the CNT and/or PVA/H₃PO₄ coating upon over stretching, though it

was still 10% higher than the initial capacitance (Figure 4f). To the best of our knowledge, the demonstrated elasticity for our supercapacitors is the highest among all the stretchable electronics with either planar or fiber structures. For comparison, the capacitance of the supercapacitor based on the CNT/PEDOT-PSS-wrapped elastic wire electrodes increased by about 6% as the strain increased from 0 to 150%, then decreased to 97% of its original capacitance when 350% strain was applied, and is attributable to deformation of the PEDOT-PSS coating upon over stretching.

The long-term elasticity of these twisted wire-shaped supercapacitors has also been investigated by repeatedly stretching the device up to 200% strain (Figure 4g). During the first few strain cycles, the capacitance increased by about 6% for the devices based on both the bare CNT-wrapped and CNT/PEDOT-PSS-wrapped elastic wire electrodes as they were stretched up to 200% strain. Thereafter, the capacitance remained stable even after one hundred cycles (Figure 4g). Clearly, therefore, these newly developed twisted wire-shaped supercapacitors are extremely elastic with a good tolerance to repeated stretching cycles even at high tensile strains, and outperformed not only the state-of-the-art fiberlike stretchable supercapacitor but also many film-type stretchable supercapacitors reported to date (see Figure S10 in the Supporting Information).

In summary, we have developed extremely stretchable wire-shaped supercapacitors, which exhibited an extremely high elasticity up to 350% strain with a high capacitance of about 8.0 F g⁻¹ at the discharge current of 0.5 A g⁻¹. By coating the CNT-wrapped elastic wire electrodes with conducting PEDOT-PSS, the device performance can be further enhanced up to 30.7 F g⁻¹, and is about two times that of the state-of-the-art fiberlike stretchable supercapacitor which can be stretched only up to 100% strain.^[27] Furthermore, our stretchable supercapacitors also showed a good long-term stretching stability. Because of the wire-shaped structure, multiple supercapacitors can be easily integrated into a single wire device to meet specific energy and power needs for practical applications. Clearly, therefore, the extremely stretchable wire-shaped supercapacitors developed in this study outperformed all the state-of-the-art stretchable elec-

tronics reported to date in terms of the elasticity and overall performance.

Received: September 23, 2014

Revised: October 15, 2014

Published online: November 17, 2014

Keywords: conductive materials · nanotubes · polymers · scanning probe microscopy · wires

-
- [1] C. Yu, C. Masarapu, J. Rong, B. Wei, H. Jiang, *Adv. Mater.* **2009**, *21*, 4793–4797.
- [2] Z. Niu, H. Dong, B. Zhu, J. Li, H. H. Hug, W. Zhou, X. Chen, S. Xie, *Adv. Mater.* **2013**, *25*, 1058–1064.
- [3] S. Xu, Y. Zhang, J. Cho, J. Lee, X. Huang, L. Jia, J. A. Fan, Y. Su, J. Su, H. Zhang, H. Cheng, B. Yu, C. Chuang, T. I. Kim, T. Song, K. Shiqeta, S. Kang, C. Dagdeviren, I. Petrov, P. V. Braun, Y. Huang, U. Paik, J. A. Rogers, *Nat. Commun.* **2013**, *4*, 1543–1550.
- [4] D. J. Lipomi, B. C. K. Tee, M. Vosgueritchian, Z. Bao, *Adv. Mater.* **2011**, *23*, 1771–1775.
- [5] G. Li, R. Zhu, Y. Yang, *Nat. Photonics* **2012**, *6*, 153–161.
- [6] T. Sekitani, H. Nakajima, H. Maeda, T. Fukushima, T. Aida, K. Hata, T. Someya, *Nat. Mater.* **2009**, *8*, 494–499.
- [7] J. A. Rogers, T. Someya, Y. Huang, *Science* **2010**, *327*, 1603–1607.
- [8] S. H. Chae, W. J. Yu, J. J. Bae, D. L. Duong, D. Perello, H. Y. Jeong, Q. H. Ta, T. H. Ly, Q. A. Yun, X. Duan, Y. H. Lee, *Nat. Mater.* **2013**, *12*, 403–409.
- [9] T. Chen, H. Peng, M. Durstock, L. Dai, *Sci. Rep.* **2014**, *4*, 3612–3618.
- [10] K. S. Kim, Y. Zhao, H. Jang, S. Y. Lee, J. M. Kim, K. S. Kim, J. H. Ahn, P. Kim, J. Y. Choi, B. H. Hong, *Nature* **2009**, *457*, 706–710.
- [11] T. Chen, Y. Xue, A. K. Roy, L. Dai, *ACS Nano* **2013**, *8*, 1039–1046.
- [12] P. Lee, J. Lee, H. Lee, J. Yeo, S. Hong, K. H. Nam, D. Lee, S. S. Lee, S. H. Ko, *Adv. Mater.* **2012**, *24*, 3326–3332.
- [13] Y. Kim, J. Zhu, B. Yeom, P. M. Di, X. Su, J. G. Kim, S. J. Yoo, C. Uher, N. A. Kotov, *Nature* **2013**, *500*, 59–63.
- [14] M. Vosgueritchian, D. J. Lipomi, Z. Bao, *Adv. Funct. Mater.* **2012**, *22*, 421–428.
- [15] Z. Xu, Z. Liu, H. Sun, C. Gao, *Adv. Mater.* **2013**, *25*, 3249–3253.
- [16] M. Zu, Q. Li, G. Wang, J. H. Byun, T. W. Chou, *Adv. Funct. Mater.* **2013**, *23*, 789–793.
- [17] J. Bae, M. K. Song, Y. J. Park, J. M. Kim, M. Liu, Z. L. Wang, *Angew. Chem. Int. Ed.* **2011**, *50*, 1683–1687; *Angew. Chem.* **2011**, *123*, 1721–1725.
- [18] J. A. Lee, M. K. Shin, S. H. Kim, H. U. Cho, G. M. Spinks, G. G. Wallace, M. D. Lima, X. Lepró, M. E. Kozlov, R. H. Baughman, S. J. Kim, *Nat. Commun.* **2013**, *4*, 2970–2977.
- [19] T. Chen, L. Qiu, Z. Yang, Z. Cai, J. Ren, H. Li, H. Lin, X. Sun, H. Peng, *Angew. Chem. Int. Ed.* **2012**, *51*, 11977–11980; *Angew. Chem.* **2012**, *124*, 12143–12146.
- [20] D. J. Lipomi, Z. Bao, *Energy Environ. Sci.* **2011**, *4*, 3314–3328.
- [21] J. Viventi, D. H. Kim, L. Vigeland, E. S. Frechette, J. A. Blanco, Y. S. Kim, A. E. Avrin, V. R. Tiruadi, S. W. Hwang, A. C. Vanleer, D. F. Wulsin, K. Davis, C. E. Gelber, L. Palmer, S. J. Van, J. Xiao, Y. Huang, D. Contreras, J. A. Rogers, B. Litt, *Nat. Neurosci.* **2011**, *14*, 1599–1605.
- [22] D. J. Lipomi, M. Vosgueritchian, B. C. Tee, S. L. Hellstrom, J. A. Lee, C. H. Fox, Z. Bao, *Nat. Nanotechnol.* **2011**, *6*, 788–792.
- [23] C. Wang, D. Hwang, Z. Yu, K. Takei, J. Park, T. Chen, B. Ma, L. Javey, *Nat. Mater.* **2013**, *12*, 899–904.
- [24] T. Someya, T. Sekitani, S. Iba, Y. Kato, H. Kawaguchi, T. Sakurai, *Proc. Natl. Acad. Sci. USA* **2004**, *101*, 9966–9970.
- [25] B. Wenger, N. Tétreault, M. E. Welland, R. H. Friend, *Appl. Phys. Lett.* **2010**, *97*, 193303.
- [26] R. F. Shepherd, F. Ilievski, W. Choi, S. A. Morin, A. A. Stokes, A. D. Mazzeo, X. Chen, M. Wang, G. M. Whitesides, *Proc. Natl. Acad. Sci. USA* **2011**, *108*, 1788–1793.
- [27] Z. Yang, J. Deng, X. Chen, J. Ren, H. Peng, *Angew. Chem. Int. Ed.* **2013**, *52*, 13453–13457; *Angew. Chem.* **2013**, *125*, 13695–13699.
- [28] H. Peng, X. Sun, F. Cai, X. Chen, Y. Zhu, G. Liao, D. Chen, Q. Li, Y. Lu, Y. Zhu, Q. Jia, *Nat. Nanotechnol.* **2009**, *4*, 738–741.
- [29] T. Chen, S. Wang, Z. Yang, Q. Feng, X. Sun, L. Li, Z. Wang, H. Peng, *Angew. Chem. Int. Ed.* **2011**, *50*, 1815–1819; *Angew. Chem.* **2011**, *123*, 1855–1859.
- [30] M. Zhang, S. Fang, A. A. Zakhidov, S. B. Lee, A. E. Aliev, C. D. Williams, K. R. Atkinson, R. H. Baughman, *Science* **2005**, *309*, 1215–1219.
- [31] X. Crispin, F. L. E. Jakobsson, A. Crispin, P. C. M. Grim, P. Andersson, A. Volodin, C. van Haesendonck, M. V. der Auweraer, W. R. Salaneck, M. Berggren, *Chem. Mater.* **2006**, *18*, 4354–4360.
- [32] D. Antiohos, G. Folkes, P. Sherrell, S. Ashraf, G. G. Wallace, P. Aitchison, A. T. Harris, J. Chen, A. I. Minett, *J. Mater. Chem.* **2011**, *21*, 15987–15994.
- [33] T. L. Kelly, K. Yano, M. O. Wolf, *ACS Appl. Mater. Interfaces* **2009**, *1*, 2536–2543.
- [34] X. Lepró, M. D. Lima, R. H. Baughman, *Carbon* **2010**, *48*, 3621–3627.
- [35] T. Chen, L. Dai, *Mater. Today* **2013**, *16*, 272–280.
- [36] M. D. Stoller, R. S. Ruoff, *Energy Environ. Sci.* **2010**, *3*, 1294–1301.
- [37] J. Zhang, X. Zhao, *ChemSusChem* **2012**, *5*, 818–841.
-